

Spectrum of low energy excitations in the vortex state: comparison of Doppler shift method to quasiclassical approach

T. Dahm, S. Graser, C. Iniotakis, and N. Schopohl

Institut für Theoretische Physik, Universität Tübingen,

Auf der Morgenstelle 14, D-72076 Tübingen, Germany

(Dated: November 4, 2018)

We present a detailed comparison of numerical solutions of the quasiclassical Eilenberger equations with several approximation schemes for the density of states of *s*- and *d*-wave superconductors in the vortex state, which have been used recently. In particular, we critically examine the use of the Doppler shift method, which has been claimed to give good results for *d*-wave superconductors. Studying the single vortex case we show that there are important contributions coming from core states, which extend far from the vortex cores into the nodal directions and are not present in the Doppler shift method, but significantly affect the density of states at low energies. This leads to sizeable corrections to Volovik's law, which we expect to be sensitive to impurity scattering. For a vortex lattice we also show comparisons with the method due to Brandt, Pesch, and Tewordt and an approximate analytical method, generalizing a method due to Pesch. These are high field approximations strictly valid close to the upper critical field B_{c2} . At low energies the approximate analytical method turns out to give impressively good results over a broad field range and we recommend the use of this method for studies of the vortex state at not too low magnetic fields.

PACS numbers: 74.20.Rp, 74.60.-w, 74.25.Bt

I. INTRODUCTION

There is now a growing number of candidate systems for unconventional or strongly anisotropic superconductivity. Besides the high- T_c cuprates, which are believed to be *d*-wave superconductors, there are indications for unconventional superconductivity in Sr_2RuO_4 ,¹ UPt_3 ,² an organic superconductor,³ the κ -(ET)₂ salts⁴ and a possible unconventional, ferromagnetically driven superconductivity is discussed in the recently found superconducting ferromagnets ZrZn_2 , URhGe and UGe_2 .⁵ Also, in MgB_2 phonon mediated, strongly anisotropic^{6,7} or two-gap scenarios⁸ have been proposed. In such systems the strong momentum dependence of the superconducting order parameter can lead to interesting new behavior, especially if there are gap nodes present at the Fermi surface. In particular, the low-energy excitations in the vortex state of such systems are expected to display unconventional behavior, as has been studied recently.^{9,10,11,12,13,14,15,16,17,18,19} In these studies the so-called Doppler shift method has been used frequently.^{15,16,17,18,19} In this method, which dates back to the early days of the theoretical study of type II superconductors,²⁰ the quasiparticle excitation energy is approximated by taking into account only the Doppler shift due to the local supercurrent flow. While this method neglects vortex core scattering and certainly is a bad approximation for conventional *s*-wave superconductors, Volovik has argued that in the case of superconductors having gap nodes, the low energy excitations are dominated by the extended quasiparticle states outside the vortex core and the Doppler shift method thus should give much better results, at least for high- κ superconductors at sufficiently low external magnetic fields.⁹ Based on the Doppler shift method, Volovik predicted

that the density of states at the Fermi level in the vortex state of a superconductor with line nodes should vary as the square root of the magnetic field, instead of the linear variation expected for a conventional superconductor. Indeed, low-temperature specific heat measurements on high- T_c cuprates have been shown to be consistent with such a field dependence.^{17,21,22,23,24}

However, the Doppler shift method is not a rigorous quasiclassical approximation in the sense of an expansion in terms of $(k_F \xi)^{-1}$, where k_F is the Fermi momentum and ξ the coherence length. Instead, the appropriate method is the solution of the Eilenberger equations for the quasiclassical propagator.^{25,26,27} Within this approach, the contribution of vortex core states and vortex core scattering is included. Of course, the Eilenberger approach requires the solution of a set of transport equations, which is more involved than the Doppler shift calculations.

In the present work we want to present detailed comparisons of Doppler shift calculations with solutions of the Eilenberger equations for *s*- and *d*-wave superconductors, in order to clarify where the Doppler shift method is a good approximation and where it fails to give quantitative agreement with the fully quasiclassical solution of the Eilenberger equations. We are also going to discuss two other approximate methods, which are expected to be good at magnetic fields close to the upper critical field B_{c2} . Indeed, in this field range it turns out that analytical results for the density of states averaged over a unit cell of the vortex lattice can be obtained, which are superior in accuracy than the Doppler shift results. A numerical solution of the Eilenberger equations is simplified considerably due to a recently found parametrization, which transforms the Eilenberger equations into scalar differential equations of the Riccati type.

In the next section we want to briefly present the Eilenberger approach and its mapping to scalar Riccati equations. We will outline, how the Doppler shift method can be obtained from the Riccati equations. Section III is devoted to the study of the local density of states for the single vortex, while in section IV we are going to present comparisons of the density of states for the vortex lattice.

II. EILENBERGER APPROACH

For a layered system with cylindrical Fermi surface and a spin-singlet superconducting order parameter the Eilenberger equation for the normal and anomalous components g and f of the quasiclassical propagator reads^{25,26}

$$\left[2 \left(i\epsilon_n + \frac{e}{c} \vec{v}_F \cdot \vec{A} \right) + i\hbar \vec{v}_F \cdot \vec{\nabla} \right] f(\vec{r}, \Theta, i\epsilon_n) = 2ig(\vec{r}, \Theta, i\epsilon_n) \Delta_0(\vec{r}, \Theta) \quad (1)$$

Here, \vec{v}_F is the Fermi velocity pointing into the direction Θ , \vec{A} is the vector potential due to the internal magnetic field within the system, ϵ_n are the fermionic Matsubara frequencies, and $\Delta_0(\vec{r}, \Theta)$ denotes the spacially varying and momentum dependent order parameter. Eq. (1) has to be supplemented by a normalization condition, which in our case reads²⁵

$$[g(\vec{r}, \Theta, i\epsilon_n)]^2 + f(\vec{r}, \Theta, i\epsilon_n) f^*(\vec{r}, \Theta + \pi, i\epsilon_n) = 1 \quad (2)$$

The normalized local density of states $N(\vec{r}, \epsilon)$ is obtained from g after an analytic continuation to real frequencies and an angular average over the Fermi surface:

$$N(\vec{r}, \epsilon) = \frac{1}{2\pi} \int_0^{2\pi} d\Theta \operatorname{Re} \{ g(\vec{r}, \Theta, i\epsilon_n \rightarrow \epsilon + i0^+) \} \quad (3)$$

It has been shown in Refs. 10,28 that Eqs. (1) and (2) can be mapped onto scalar Riccati equations along real space trajectories $\vec{r}(x)$ running parallel to the direction of the Fermi velocity, if one introduces two scalar complex quantities $a(x)$ and $b(x)$

$$g(\vec{r}(x)) = \frac{1 - a(x)b(x)}{1 + a(x)b(x)} \quad f(\vec{r}(x)) = \frac{2ia(x)}{1 + a(x)b(x)} \quad (4)$$

where $a(x)$ and $b(x)$ obey the following Riccati equations

$$\hbar v_F \frac{\partial}{\partial x} a(x) + [2\tilde{\epsilon}_n(x) + \Delta^\dagger(x)a(x)] a(x) - \Delta(x) = 0 \quad (5)$$

$$\hbar v_F \frac{\partial}{\partial x} b(x) - [2\tilde{\epsilon}_n(x) + \Delta(x)b(x)] b(x) + \Delta^\dagger(x) = 0 \quad (6)$$

Here, $i\tilde{\epsilon}_n(x) = i\epsilon_n + \frac{e}{c} \vec{v}_F \cdot \vec{A}(x)$. The initial values for the two quantities $a(x)$ and $b(x)$ in the bulk superconductor

have to be taken as

$$a(-\infty) = \frac{\Delta(-\infty)}{\epsilon_n + \sqrt{\epsilon_n^2 + |\Delta(-\infty)|^2}} \quad (7)$$

$$b(+\infty) = \frac{\Delta^\dagger(+\infty)}{\epsilon_n + \sqrt{\epsilon_n^2 + |\Delta(+\infty)|^2}} \quad (8)$$

Once the order parameter field $\Delta_0(\vec{r}, \Theta)$ and the vector potential $\vec{A}(\vec{r})$ are known, the initial value problem for the scalar differential equations (5) and (6) can be solved by standard numerical techniques (adaptive Runge-Kutta method for example). For a homogeneous bulk superconductor one confirms that Eqs. (7) and (8) indeed fulfil Eqs. (5) and (6). In order to find the local density of states Eq. (3) for a given point \vec{r} and energy ϵ it is necessary to solve the Riccati equations (5) and (6) for a bundle of trajectories running through the point \vec{r} with different angles Θ .

It is instructive to see how the Doppler shift method can be obtained from Eq. (5). For that purpose we first decompose the order parameter $\Delta(x)$ into amplitude and phase via

$$\Delta(x) = \bar{\Delta}(x) e^{i\Phi(x)} \quad (9)$$

Introducing the function

$$\bar{a}(x) = a(x) e^{-i\Phi(x)} \quad (10)$$

one arrives at an equation for \bar{a} :

$$\hbar v_F \frac{\partial}{\partial x} \bar{a}(x) + [2\epsilon_n + 2i\vec{v}_F \cdot m\vec{v}_s(x) + \bar{\Delta}(x)\bar{a}(x)] \bar{a}(x) - \bar{\Delta}(x) = 0 \quad (11)$$

where $\vec{v}_s(x) = \frac{1}{2m} (\hbar \vec{\nabla} \Phi(x) - \frac{2e}{c} \vec{A}(x))$ is nothing but the gauge invariant superfluid velocity of the supercurrent field distribution. If we now neglect the spacial derivative $\frac{\partial}{\partial x} \bar{a}(x)$ we find from Eq. (11)

$$\bar{a}(x) = \frac{\bar{\Delta}(x)}{\bar{\epsilon}_n(x) + \sqrt{\bar{\epsilon}_n(x)^2 + \bar{\Delta}(x)^2}} \quad (12)$$

with $\bar{\epsilon}_n(x) = \epsilon_n + i m \vec{v}_F \cdot \vec{v}_s(x)$. Thus, we rediscover the bulk result apart from a Doppler shift in energy. If we set $\bar{\Delta}(x)$ equal to its homogeneous bulk value using Eqs. (3) and (4) we just obtain the usual Doppler shift equation¹⁵

$$N_{\text{DS}}(\vec{r}, \epsilon) = \frac{1}{2\pi} \int_0^{2\pi} d\Theta \operatorname{Re} \left\{ \frac{|\epsilon - m\vec{v}_F \cdot \vec{v}_s(\vec{r})|}{\sqrt{(\epsilon - m\vec{v}_F \cdot \vec{v}_s(\vec{r}))^2 - |\Delta(\Theta)|^2}} \right\} \quad (13)$$

From this derivation we learn that the Doppler shift method neglects the gradient term in the Eilenberger equations. This neglection is expected to be a reasonable approximation as long as the Doppler shift energy $m\vec{v}_F \cdot \vec{v}_s(\vec{r})$ is small compared to the local gap energy $\Delta(\vec{r}, \Theta)$. As is well known, this approximation fails close to the vortex cores, where the superfluid velocity diverges. However, as we will see later, this approximation also fails in the vicinity of gap nodes of $\Delta(\vec{r}, \Theta)$.

III. THE SINGLE PHASE VORTEX

In order to make quantitative comparisons between the Doppler shift method and the Eilenberger approach, we first want to study the single vortex case. In particular, we restrict ourselves to the pure 'phase vortex' for which the amplitude of the order parameter $\Delta(\Theta)$ is assumed to be constant as a function of \vec{r} and only its phase is varying. For a d -wave superconductor taking the magnetic field along the c-axis direction we then have

$$\Delta(\vec{r}, \Theta) = \Delta_0 \cos(2\Theta) e^{i\phi} \quad (14)$$

where ϕ denotes the polar angle of \vec{r} . We choose this model for the vortex, because it should be the 'best case' for the Doppler shift method, since it neglects any spatial variation of the amplitude of the gap. Such a model for the vortex is expected to be reasonable for a high- κ superconductor at low magnetic fields of the order of the lower critical field H_{c1} . Although this phase vortex does not possess a core in the usual sense, we will see that there still exists a core region in the Eilenberger approach, which is due to the gradient term. One observes that the gradient term introduces a length scale $\xi = \hbar v_F / \Delta$ into the problem, even if the amplitude Δ itself does not vary. For the single vortex the Doppler shift energy diverges like r^{-1} and we have

$$m\vec{v}_F \cdot \vec{v}_s(\vec{r}) = \frac{\hbar}{2r} \vec{v}_F \cdot \hat{e}_\phi = \frac{\hbar v_F}{2r} \sin(\Theta - \phi) \quad (15)$$

where \hat{e}_ϕ is the unit vector in ϕ -direction. This equation holds as long as r is smaller than the penetration depth. Otherwise the screening of the magnetic field has to be taken into account as well.

We have calculated the local density of states for the Doppler shift method using Eqs. (13) and (15). The local density of states for the Eilenberger approach is obtained from Eqs. (3) and (4) numerically using the Riccati method outlined above. In order to facilitate the solution a small imaginary part $\delta \leq 0.01\Delta_0$ has been added to the energies on the real axis.

In Figs. 1 and 2 we are showing our results for the energy dependence of the local density of states for a d -wave superconducting state. Here and in the following the density of states is normalized to the normal state value. In Fig. 1(a) and (b) the results in an angular direction of $\phi = 0$ are shown for distances $r = 1$ and $r = 3$ from the vortex center (in units of the coherence length ξ). Figs. 2(a) and (b) show the corresponding results for an angular direction of $\phi = \pi/4$ (nodal direction). As becomes clear from these plots, the Doppler shift method gives reasonable results at sufficient high energy and also becomes better at distances further away from the vortex center. However, at distances from the vortex of the order of the coherence length the Doppler shift fails to give the position of the peaks correctly, which result from core state contributions or scattering resonances.^{10,29} The satellite peaks in the Doppler-shift

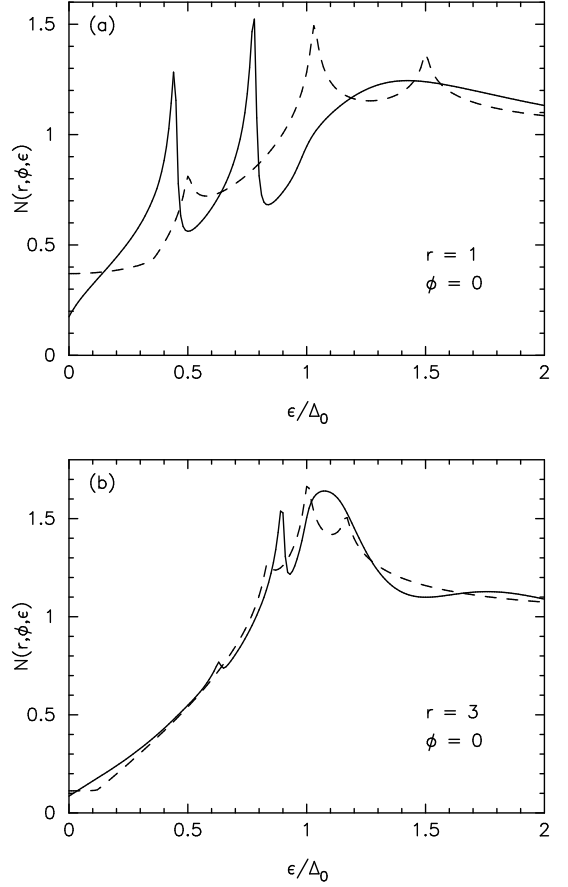


FIG. 1: Local density of states in the vicinity of a d -wave phase vortex at distances (a) $r = 1$ and (b) $r = 3$ (in units of the coherence length) from the vortex center in the antinodal direction $\phi = 0$. The dashed line shows the result from the Doppler shift calculation, while the solid line is the result from a numerical solution of the Eilenberger equations.

method seen in Figs. 1 and 2 appear at the Doppler shifted gap energy, as has been discussed recently in Ref. 15. A discussion of the position of the peaks for the d -wave vortex within the quasiclassical approximation can be found in Refs. 10,29.

It has been noted earlier that in a d -wave vortex the core states are not truly localized.^{30,31} Nevertheless, they give important contributions to the local density of states, which are not captured by the Doppler shift method, but are present in the numerical solution of Eilenberger's equations. We emphasize that these resonances are still present, although our phase vortex does not possess a variation of the magnitude of the gap. Thus, they cannot easily be understood as 'bound states' in the potential well of the gap at the vortex core. Instead, these resonances arise due to scattering of the quasiparticles at the phase gradient around the vortex center and thus can be interpreted as Andreev scattering resonances. For comparison, we also did calculations where we multiplied Eq. (14) by $\tanh(r/\xi_c)$, where ξ_c is

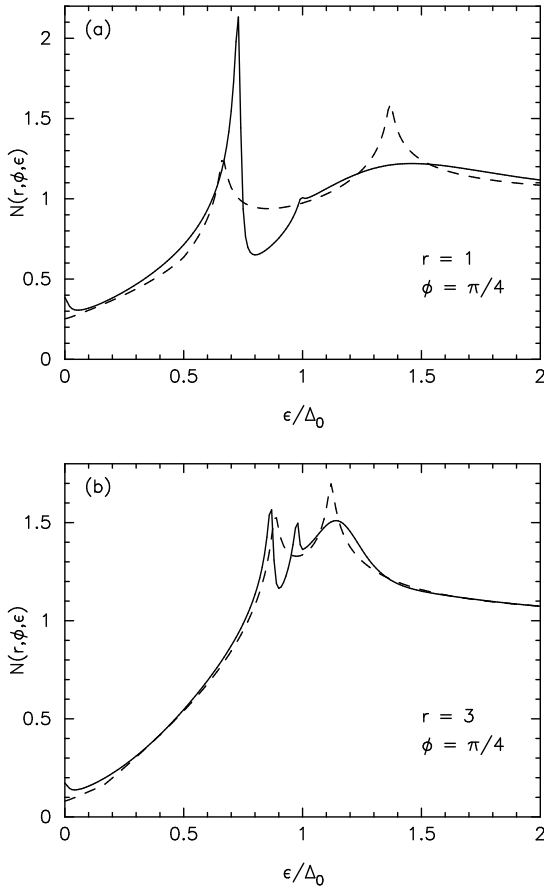


FIG. 2: Same as Fig. 1, but in the nodal direction $\phi = \pi/4$ from the vortex center.

an adjustable parameter independent of ξ , which allows us to smoothly cross over from a vortex possessing a core in the usual sense to our phase vortex, taking the limit $\xi_c \rightarrow 0$. These calculations confirm that the core state contributions do not disappear in this limit, but instead smoothly evolve into the peaks seen in Figs. 1 and 2.

Even some distance away from the vortex center, the Doppler shift does not give the correct behavior at low energies, however. As can be seen in Fig. 2(a) and (b), there is a small peak at low energies in the local density of states in the quasiclassical solution. This peak is mainly visible in the vicinity of the nodal direction $\phi = \pi/4$, as has been noted before,²⁹ and is due to extended core states, which can 'leak out' of the vortex core region due to the nodes in the gap function. This effect is also not present in the Doppler shift calculation.

This becomes more transparent from Fig. 3, where we show the zero energy local density of states at a distance $r = 5$ from the vortex center as a function of polar angle ϕ . The symbols show the results from our numerical solution of Eilenberger's equations, open circles for an imaginary part of $\delta = 0.01$ and solid circles for $\delta = 0.001$ (in units of Δ_0). The dashed line shows the Doppler shift result. (A discussion of the solid line is found be-

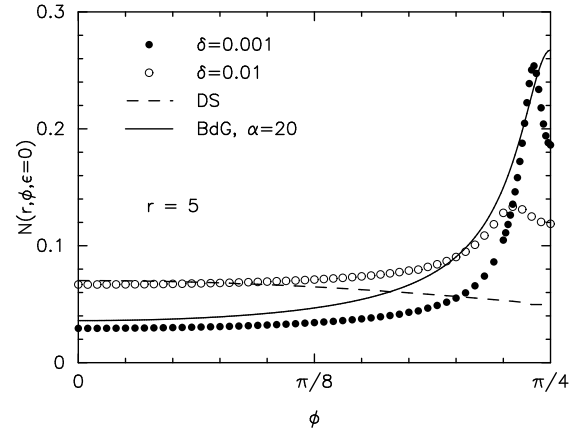


FIG. 3: Zero energy local density of states at a distance of $r = 5$ from the vortex center plotted as a function of polar angle ϕ . The circles are numerical results obtained from the solution of Eilenberger's equations using different imaginary parts: $\delta = 0.001$ (full circles) and $\delta = 0.01$ (open circles). The dashed line is the result obtained from the Doppler shift (DS) method. The solid line shows the angular dependence expected from a solution of the Bogoliubov-de Gennes (BdG) equations linearized around the gap nodes due to Mel'nikov.³²

low). From this plot it becomes clear that the solution of Eilenberger's equations yields increased contributions to the local density of states at zero energy especially close to the nodal direction $\phi = \pi/4$, which the Doppler shift method is not able to capture. We can trace back these increased contributions to quasiparticle trajectories passing near by the vortex center with a momentum direction close to the nodal direction $\Theta = \pi/4$ by looking at the momentum resolved local density of states $N(r, \phi, \Theta, \epsilon) = \text{Re} \{g(r, \phi, \Theta, \epsilon)\}$. On these particular trajectories the gap is small and the corresponding wavefunction of the quasiparticle extends very far, 'leaking out' of the core region. These nonlocal effects are missed by the Doppler shift method, since it only knows about the local supercurrent flow. As Fig. 3 shows, this effect strongly depends on the imaginary part δ chosen. It is clear that δ introduces a finite mean free path into the problem, which limits the extend to which these quasiparticle states can contribute to the local density of states far from the vortex core. Thus, one should expect that this effect is sensitive to impurity scattering.

One notes that in Fig. 3 the results from Eilenberger's equations display peaks slightly off the $\phi = \pi/4$ direction. The position of the peaks depends on δ and moves closer to $\pi/4$ when δ is reduced. The suppression directly at $\pi/4$ is due to the presence of the d -wave gap node in this direction, because a trajectory passing through the vortex center in this direction does not 'see' a gap and thus no resonant Andreev scattering takes place. (For comparison see also Fig. 8d in Ref. 29). We observe that the main contribution to the local density of states

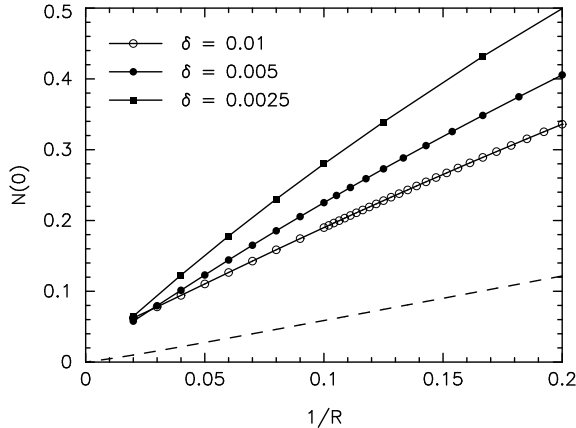


FIG. 4: Average density of states within a circle of radius R (in units of the coherence length ξ) around the vortex plotted as a function of $1/R$. The dashed line is Volovik's result obtained from the Doppler shift method. The symbols are numerical results obtained from a solution of Eilenberger's equations using different imaginary parts: $\delta = 0.01$ (open circles), $\delta = 0.005$ (full circles), and $\delta = 0.0025$ (full squares). Here, δ is measured in units of the gap amplitude Δ_0 .

in this case is coming from trajectories slightly off the $\pi/4$ direction, depending on the momentum width induced by δ .

This effect also has important consequences for the magnetic field dependence of the density of states at zero energy. In Fig. 4 we show the density of states averaged over a circle of radius R around the vortex center as a function of $1/R$, which at low fields and for high κ superconductors is proportional to the square-root of the magnetic field. The Doppler shift method yields a square-root dependence of the density of states as a function of magnetic field (a linear variation as a function of $1/R$), which has been noted first by Volovik.⁹ However, the quasiclassical solution leads to important deviations from this law. First of all, the slope of these curves is much higher, and secondly this effect is very sensitive to the imaginary part chosen in the calculation, as is clear from the discussion above. While we believe that the field dependence of these curves will probably not be distinguishable experimentally from the square-root field dependence, a systematic study of the influence of impurity content on the field dependence of the specific heat at low temperatures might be able to detect the sensitivity of the slope to impurity scattering and would be a valuable confirmation of the presence of these extended core states.

Since we are working here with a quasiclassical approximation one might ask, how important quantum effects like the Aharonov-Bohm effect might be on these extended core states. Indeed, the Aharonov-Bohm effect for a d -wave vortex has been studied recently by Mel'nikov within a solution of the Bogoliubov-de Gennes equations linearized around the gap nodes.³² Within this

quantum mechanical calculation Mel'nikov showed that the angular dependence of the zero energy density of states far from the vortex core is determined by the Dirac cone anisotropy $\alpha = v_F/v_\Delta$, where v_Δ is the quasi-particle velocity tangential to the Fermi surface at the node, which is given by the slope of the gap (in our case $v_\Delta = 2\Delta_0/\hbar k_F$ and thus $\alpha = k_F\xi/2$). For the angular dependence Mel'nikov found the expression³²

$$N\left(r, \phi - \frac{\pi}{4}, \epsilon = 0\right) = \frac{4 \xi}{\pi r} \left\{ \frac{1}{\sqrt{\alpha^2 \cos^2 \phi + \sin^2 \phi}} + \frac{1}{\sqrt{\alpha^2 \sin^2 \phi + \cos^2 \phi}} \right\} \quad (16)$$

(Note, that in Ref. 32 the nodal direction corresponds to $\phi = 0$. Therefore, we are shifting this expression here by $\pi/4$. The prefactor $4/\pi$ can be found from Mel'nikov's result normalizing it to the normal density of states). For comparison this angular dependence is shown in Fig. 3 for $\alpha = 20$ as the solid line. The angular dependence becomes more pronounced for higher values of α , but estimates from thermal conductivity measurements on high- T_c cuprates indicate anisotropies in the range $\alpha \sim 15 - 20$.³³ Clearly, the contribution from the extended core states is contained in both the quantum mechanical and the quasiclassical calculation. Note, that the full quantum mechanical information about the particle-hole coherence along the classical trajectories is contained in the quasiclassical approach (while the quantization perpendicular to the trajectories is neglected). Our quasiclassical approach corresponds to taking the limit $2\alpha = k_F\xi \rightarrow \infty$, but does not depend on a linearization around the gap node. From the comparison in Fig. 3 we expect that full quantum interference, i.e. interference of quasiparticles running classically different ways around the vortex line, will limit (via the Dirac cone anisotropy) the angular dependence of the density of states. But this comparison also shows that a very pure sample is needed, if one wants to observe these quantum mechanical effects, since at shorter mean free paths the angular dependence is expected to be limited by the impurity scattering rate.

IV. VORTEX LATTICE

We now want to focus our attention on the density of states in the vortex lattice. In the vortex lattice, the order parameter profile as well as the superfluid flow around the vortices has to be modified as compared to the single vortex case in Eqs. (14) and (15). Specifically, here we will use Abrikosov's wavefunction, which is the exact solution close to the upper critical field B_{c2} . An arbitrary vortex lattice Λ can be spanned by two lattice vectors $\vec{R}_1 = (\omega_1, 0)$ and $\vec{R}_2 = (\text{Re } \omega_2, \text{Im } \omega_2)$, where we combined the x- and y-component of \vec{R}_2 into the complex quantity ω_2 and we have chosen the x-axis into the \vec{R}_1 direction. Without loss of generality we may assume

$\omega_1 > 0$ and $\text{Im } \omega_2 > 0$. Using the quantities ω_1 and ω_2 we can generalize Abrikosov's wavefunction in the following form:

$$\psi_\Lambda(x, y) = \frac{1}{\mathcal{N}} \sum_{n=-\infty}^{\infty} \exp \left[\frac{\pi(ixy - y^2)}{\omega_1 \text{Im } \omega_2} + i\pi n + \frac{i\pi(2n+1)}{\omega_1} (x + iy) + i\pi \frac{\omega_2}{\omega_1} n(n+1) \right] \quad (17)$$

where $\mathcal{N} = \left[\frac{\omega_1}{2 \text{Im } \omega_2} \exp \left(\pi \frac{\text{Im } \omega_2}{\omega_1} \right) \right]^{1/4}$ is a normalization factor such that $|\psi_\Lambda|^2$ averaged over a unit cell C_Λ of the vortex lattice becomes unity. For a square lattice we have $\omega_2 = i\omega_1$, while for a triangular lattice $\omega_2 = \frac{1+i\sqrt{3}}{2}\omega_1$. The average magnetic field \vec{B}_{av} in the superconductor points into the z -direction and the gauge has been chosen such that the vector potential obeys the relation

$$\vec{A} = -\frac{1}{2}\vec{r} \times \vec{B}_{\text{av}} \quad (18)$$

Due to the flux quantization the average magnetic field is related to the area of the unit cell of the vortex lattice yielding the relation $B_{\text{av}} = \frac{hc}{2e\omega_1 \text{Im } \omega_2}$. The superfluid velocity field $\vec{v}_s(\vec{r})$ for the Doppler shift calculation can then be obtained from Eq. (17) using the relation

$$\begin{aligned} \vec{v}_s(\vec{r}) &= \frac{\hbar}{4mi} \frac{\psi_\Lambda^* \vec{\nabla} \psi_\Lambda - \psi_\Lambda \vec{\nabla} \psi_\Lambda^*}{|\psi_\Lambda|^2} - \frac{e}{mc} \vec{A} \quad (19) \\ &= \frac{\hbar}{2m} \left\{ \frac{\text{Im} [\psi_\Lambda^* \vec{\nabla} \psi_\Lambda]}{|\psi_\Lambda|^2} - \frac{\pi}{\omega_1 \text{Im } \omega_2} \begin{pmatrix} -y \\ x \end{pmatrix} \right\} \end{aligned}$$

Due to the n^2 term in the exponent the sum in Eq. (17) quickly converges and only a few terms are sufficient to find $\psi_\Lambda(x, y)$. For our numerical solution of the Eilenberger equations for a d -wave superconductor we then use the order parameter

$$\Delta(\vec{r}, \Theta) = \Delta_0 \cos(2\Theta) \psi_\Lambda(\vec{r}) \quad (20)$$

When solving the Riccati equations Eqs. (5) and (6) for the vortex lattice we have to ensure that a solution periodic in the lattice is found. We achieve that by utilizing our small imaginary part δ for the energies. For a given point in space and momentum we choose the starting point of the corresponding trajectory a long distance of order $1/\delta$ unit cells away. This gives the solution a distance to relax to the periodic solution sought, where the relaxation is provided by δ . We have explicitly checked that the result is periodic and doesn't change anymore, if we repeat the calculation with a longer trajectory.

A. An approximate analytical solution

At high magnetic fields close to the upper critical field B_{c2} it is possible to obtain analytic results for

the density of states averaged over a unit cell of the vortex lattice, generalizing a method due to Pesch,³⁴ which has been used recently also for the study of d -wave superconductors.³⁵ These analytic results can be obtained as follows. The first step is to replace the function g on the right hand side in Eq. (1) by its value averaged over a unit cell of the vortex lattice. This approximation is certainly valid close to the upper critical field, because there g does not vary strongly within a unit cell. Then we have

$$L(\vec{r}, \Theta, i\epsilon_n) = 2\langle g(\vec{r}, \Theta, i\epsilon_n) \rangle_{C_\Lambda} \Delta(\vec{r}, \Theta) \quad (21)$$

where $\langle \dots \rangle_{C_\Lambda}$ denotes an average over a unit cell of \vec{r} and the operator L is given by

$$L = L(\Theta) = 2 \left(\epsilon_n - i \frac{e}{c} \vec{v}_F(\Theta) \cdot \vec{A} \right) + \hbar \vec{v}_F(\Theta) \cdot \vec{\nabla} \quad (22)$$

Assuming without loss of generality that $\epsilon_n > 0$ Eq. (21) can be inverted using the operator identity³⁶

$$L^{-1} = \int_0^\infty ds e^{-sL} \quad (23)$$

Since $\langle g \rangle_{C_\Lambda}$ does not depend on the variable \vec{r} anymore, L only acts upon Δ and we find

$$f(\vec{r}, \Theta, i\epsilon_n) = 2\langle g(\vec{r}, \Theta, i\epsilon_n) \rangle_{C_\Lambda} \int_0^\infty ds e^{-sL} \Delta(\vec{r}, \Theta) \quad (24)$$

Using the normalization condition Eq. (2) we can calculate the cell average of the square of g :

$$\begin{aligned} \langle g^2(\vec{r}, \Theta, i\epsilon_n) \rangle_{C_\Lambda} &= 1 - \langle f(\vec{r}, \Theta, i\epsilon_n) f^*(\vec{r}, \Theta + \pi, i\epsilon_n) \rangle_{C_\Lambda} \\ &= 1 - \langle g(\vec{r}, \Theta, i\epsilon_n) \rangle_{C_\Lambda}^2 P_\Lambda(\Theta, i\epsilon_n) \end{aligned} \quad (25)$$

where

$$\begin{aligned} P_\Lambda(\Theta, i\epsilon_n) &= 4 \int_0^\infty ds_- \int_0^\infty ds_+ \\ &\quad \langle (e^{-s_+ L} \Delta(\vec{r}, \Theta)) (e^{-s_- L} \Delta^\dagger(\vec{r}, \Theta + \pi)) \rangle_{C_\Lambda} \end{aligned} \quad (26)$$

Here we have used the relation $g^\dagger(\Theta + \pi) = g(\Theta)$ and inversion symmetry $L^\dagger(\Theta + \pi) = L(\Theta)$. Close to the upper critical field we may assume as a second step that

$$\langle g^2(\vec{r}, \Theta, i\epsilon_n) \rangle_{C_\Lambda} = \langle g(\vec{r}, \Theta, i\epsilon_n) \rangle_{C_\Lambda}^2 \quad (27)$$

which amounts to neglecting spacial fluctuations of g . Using this approximation Eq. (25) becomes a closed equation for $\langle g \rangle_{C_\Lambda}$ and we finally find

$$\langle g(\vec{r}, \Theta, i\epsilon_n) \rangle_{C_\Lambda} = \frac{1}{\sqrt{1 + P_\Lambda(\Theta, i\epsilon_n)}} \quad (28)$$

As it turns out, Eq. (26) can be evaluated analytically for the Abrikosov vortex lattice Eq. (17). After some algebra³⁶ we find

$$P_\Lambda(\Theta, i\epsilon_n) = \frac{2\Delta_0^2 \cos^2(2\Theta)}{\epsilon_n^2} z^2 [1 - \sqrt{\pi} z w(iz)] \quad (29)$$

where

$$z = \frac{\sqrt{2\omega_1 \text{Im } \omega_2} \epsilon_n}{\sqrt{\pi} v_F \hbar} \quad (30)$$

Here, the function w is Dawson's integral and is related to the complement of the Error function via

$$w(iz) = \frac{1}{i\pi} \int_{-\infty}^{\infty} \frac{e^{-t^2} dt}{t - iz} = e^{z^2} \text{erfc}(z) \quad (31)$$

Some properties of this function can be found in Ref. 37. We can make these equations a little bit more transparent, if we introduce two length scales: the coherence length $\xi = v_F \hbar / \Delta_0$ and $a_\Lambda^2 = \omega_1 \text{Im } \omega_2 = \Phi_0 / B_{\text{av}}$ with Φ_0 being the flux quantum. a_Λ^2 is the area of a unit cell of the vortex lattice and for a square lattice a_Λ is just the distance between neighboring vortices. We remark that also the coherence length ξ depends on magnetic field, since Δ_0 has to be determined from the gap equation in the presence of the field. Expressed in these quantities we have

$$z = \sqrt{\frac{2}{\pi}} \frac{a_\Lambda}{\xi} \frac{\epsilon_n}{\Delta_0} \quad (32)$$

To obtain the cell average of the density of states, Eq. (28) has to be integrated over the angle Θ and analytically continued to real frequencies $i\epsilon_n \rightarrow \epsilon + i0^+$. Since P_Λ only depends on Θ via the $\cos^2(2\Theta)$ term, the angular integral is just a complete elliptical integral and we find the analytical result

$$\begin{aligned} N(\epsilon) &= \frac{1}{2\pi} \int_0^{2\pi} d\Theta \text{Re} \langle g(\vec{r}, \Theta, i\epsilon_n \rightarrow \epsilon + i0^+) \rangle_{C_\Lambda} \\ &= \frac{2}{\pi} \text{Re} \{K(k)\} \end{aligned} \quad (33)$$

with

$$k^2 = -\frac{4}{\pi} \frac{a_\Lambda^2}{\xi^2} \left[1 + i\sqrt{2} \frac{a_\Lambda}{\xi} \frac{\epsilon}{\Delta_0} w \left(\sqrt{\frac{2}{\pi}} \frac{a_\Lambda}{\xi} \frac{\epsilon}{\Delta_0} \right) \right] \quad (34)$$

For comparison, for an *s*-wave superconductor the $\cos^2(2\Theta)$ factor in Eq. (29) has to be dropped and we just find

$$N(\epsilon) = \text{Re} \left\{ \frac{1}{\sqrt{1 - k^2}} \right\} \quad (35)$$

It is instructive to consider the low and high field limits of these expressions. At high magnetic field B_{av} the coherence length ξ diverges. In this limit $k \rightarrow 0$ and we find the normal state result $N(\epsilon) \rightarrow 1$ for both *s*- and *d*-wave superconductor as one should expect. For low magnetic fields ξ becomes constant, but a_Λ diverges. In this limit one can use the asymptotic expansion of Dawson's integral³⁷

$$1 - \sqrt{\pi} z w(iz) \sim \frac{1}{2z^2} \quad (36)$$

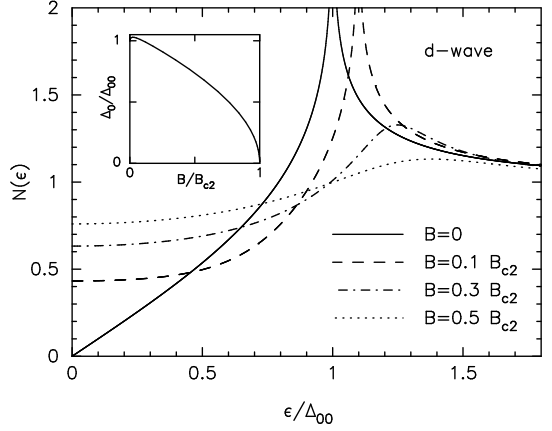


FIG. 5: Average density of states in the vortex state of a *d*-wave superconductor calculated using the analytical formula Eq. (33) for different field strengths: $B_{\text{av}} = 0$ (solid line), $B_{\text{av}} = 0.1B_{\text{c}2}$ (dashed line), $B_{\text{av}} = 0.3B_{\text{c}2}$ (dashed-dotted line), and $B_{\text{av}} = 0.5B_{\text{c}2}$ (dotted line). The energy is normalized to the gap value at zero field and temperature $\Delta_{00} = \Delta_0(T = 0, B = 0)$. The inset shows the field dependence of the zero temperature gap Δ_0/Δ_{00} .

Then we have $k^2 \sim \Delta_0^2/\epsilon^2$. Inserting this into Eqs. (33) and (35) we just rediscover the zero field density of states of the *d*- and *s*-wave superconductor, respectively. It is interesting to note that this high field approximation also appears to give the correct zero field limit.

In Fig. 5 we show the density of states calculated from Eq. (33) for different magnetic fields at zero temperature. In order to find the appropriate value of a_Λ/ξ for a given field and temperature, it is necessary to solve the gap equation in order to find $\Delta_0(T, B_{\text{av}})$. Using the approximation Eq. (24) the gap equation for the *d*-wave case can be cast into the form

$$\begin{aligned} \ln \left(\frac{T}{T_c} \right) &= \\ T \sum_{\epsilon_n} \int_0^{2\pi} d\Theta \frac{2 \cos^2(2\Theta)}{\epsilon_n} &\left\{ \frac{\sqrt{\pi} z w(iz)}{\sqrt{1 + P_\Lambda(\Theta, i\epsilon_n)}} - 1 \right\} \end{aligned} \quad (37)$$

with z depending on ϵ_n and B_{av} via Eq. (30). The angular integration over Θ can even be further reduced to complete elliptical integrals, if desired. The field dependence of the gap at zero temperature obtained from this equation is shown in the inset to Fig. 5. The energy scale in Fig. 5 has been normalized to the zero field and temperature value of the gap $\Delta_{00} = \Delta_0(T = 0, B_{\text{av}} = 0)$. In the inset it can be noted that the gap Δ_0 as a function of magnetic field rises above Δ_{00} at low field before reaching its zero field value Δ_{00} at $B_{\text{av}} = 0$. This is a property of Eq. (37) and we attribute it to the fact that the approximation used in the present section is valid only at high field and at zero field. Fig. 5 shows that, although the gap closes as a function of field B_{av} , the peaks in the density of states move upwards in energy. This means

that in the vortex state the peak-to-peak distance in the density of states is not an appropriate measure of the energy gap Δ_0 anymore. This fact is important to realize in interpretation of tunneling spectra in the vortex state, for example.

B. The approximation due to Brandt, Pesch, and Tewordt

In the literature there exists another approximation for the average density of states in type II superconductors at high magnetic fields, which is due to Brandt, Pesch, and Tewordt³⁸ and also has been used recently to study unconventional superconductors.^{39,40} In their original paper these authors derived their method from Gorkov's equation.⁴¹ We discovered a method to re-derive their results from the Eilenberger equation using the Riccati equations (5) and (6), which we want to briefly sketch here.

Instead of replacing the function g by its average value in Eq. (1) we can use an approximation similar in spirit in the Riccati equations (5) and (6), linearizing them by replacing the terms $\Delta^\dagger a$ and Δb by their averages over a unit cell. For the function a one obtains the equation

$$\bar{L}a(\vec{r}, \Theta, i\epsilon_n) = \Delta(\vec{r}, \Theta) \quad (38)$$

where \bar{L} is just the operator in Eq. (22), except that ϵ_n now has to be replaced by

$$\bar{\epsilon}_n = \epsilon_n + \frac{1}{2}\langle\Delta^\dagger a\rangle_{C_\Lambda} \quad (39)$$

Eq. (38) can be inverted the same way as above and after some algebra we obtain for the average $\langle\Delta^\dagger a\rangle_{C_\Lambda}$:

$$\begin{aligned} \langle\Delta^\dagger a\rangle_{C_\Lambda} &= \int_0^\infty ds \langle\Delta^\dagger(\vec{r}, \Theta)e^{-s\bar{L}}\Delta(\vec{r}, \Theta)\rangle_{C_\Lambda} \\ &= \Delta_0 \cos^2(2\Theta) \frac{a_\Lambda}{\sqrt{2}\xi} w(i\bar{z}) = 2(\bar{\epsilon}_n - \epsilon_n) \end{aligned} \quad (40)$$

where now

$$\bar{z} = \frac{\sqrt{2\omega_1 \text{Im } \omega_2} \bar{\epsilon}_n}{\sqrt{\pi} v_F \hbar} = \sqrt{\frac{2}{\pi}} \frac{a_\Lambda}{\xi} \frac{\bar{\epsilon}_n}{\Delta_0} \quad (41)$$

Eq. (40) is an implicit equation for $\bar{\epsilon}_n$ or equivalently for \bar{z} and can be written in the form

$$i\bar{z} = \sqrt{\frac{2}{\pi}} \frac{a_\Lambda}{\xi} \frac{i\epsilon_n}{\Delta_0} + i \cos^2(2\Theta) \frac{a_\Lambda^2}{2\sqrt{\pi}\xi^2} w(i\bar{z}) \quad (42)$$

From the inversion of Eq. (38) and the equivalent one for the function b one can also obtain the cell average of the product ab :

$$\langle ab\rangle_{C_\Lambda} = \cos^2(2\Theta) \frac{a_\Lambda^2}{\pi\xi^2} [1 - \sqrt{\pi}\bar{z} w(i\bar{z})] \quad (43)$$

Using this result we can obtain an approximation for the cell average of the propagator g using Eq. (4)

$$\begin{aligned} \langle g(\vec{r}, \Theta, i\epsilon_n)\rangle_{C_\Lambda} &\approx \frac{2}{1 + \langle ab\rangle_{C_\Lambda}} - 1 \\ &= \frac{2}{1 + \cos^2(2\Theta) \frac{a_\Lambda^2}{\pi\xi^2} [1 - \sqrt{\pi}\bar{z} w(i\bar{z})]} - 1 \end{aligned} \quad (44)$$

where \bar{z} has to be obtained from a solution of Eq. (42) for each ϵ_n and Θ . The set of equations (42) and (44) just corresponds to Eqs. (18) and (16) in Ref. 38. (The parameter Λ in that work corresponds to $a_\Lambda/\sqrt{2\pi}$ in our case).

This derivation shows that the approximation due to Brandt, Pesch, and Tewordt can also be justified from quasiclassical Eilenberger theory. However, in contrast to the approximate analytical method derived in the previous subsection, here one has to solve a nonlinear implicit equation, which makes the calculation of the density of states more difficult. An expansion of Eqs. (44) and (28) in terms of Δ_0 shows that both methods give the same result up to order $|\Delta_0|^3$.

C. Comparison with numerical results

We now want to present a comparison of the four methods outlined above: the Doppler shift method (DS), the approximate analytical solution (AA), the method due to Brandt, Pesch, and Tewordt (BPT), and a full numerical solution of Eilenberger's equations (EE) using the Riccati equations. In all four cases we will base our calculations on an Abrikosov square lattice. However, the results do not differ very much, if a triangular lattice is used. In fact, the density of states within the methods AA and BPT does not depend on the lattice structure, as is clear from the derivation above.

In the following we will compare our results using the parameter ξ/a_Λ . This parameter is a measure of the average magnetic field B_{av} inside the superconductor and at low field strengths $\xi/a_\Lambda \propto \sqrt{B_{av}}$. At higher field strengths its field dependence has to be determined from a solution of the gap equation, because ξ depends on Δ_0 , which decreases with increasing field. From such a solution we have determined that $\xi/a_\Lambda = 1$ corresponds to about $B_{av} \approx 0.5B_{c2}$ and $\xi/a_\Lambda = 0.2$ corresponds to about $B_{av} \approx 0.04B_{c2}$ at zero temperature.

In Fig. 6 we show the cell average of the density of states as a function of energy for the four methods. In Fig. 6(a) the comparison for $\xi/a_\Lambda = 1$ is shown, Fig. 6(b) shows the results for $\xi/a_\Lambda = 0.2$. At high magnetic field ($\xi/a_\Lambda = 1$) the numerical solution of the Eilenberger equations (EE, black dots), and the methods AA (solid line) and BPT (dotted line) are all in very close agreement with each other, the approximate analytical (AA) result being somewhat closer to the numerical solution. The Doppler shift method (dashed line), however, strongly deviates from these results. This result is

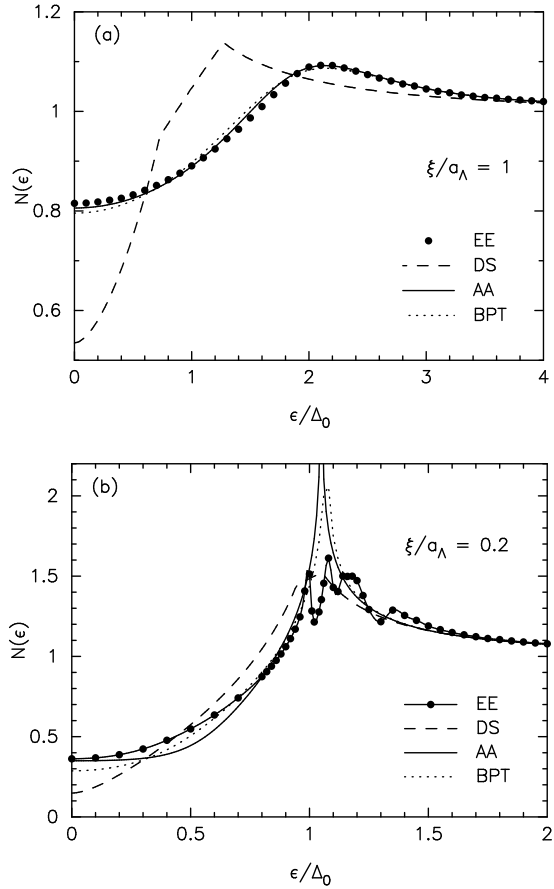


FIG. 6: Energy dependence of the density of states averaged over a unit cell of the vortex lattice for (a) $\xi/a_\Lambda = 1$ and (b) $\xi/a_\Lambda = 0.2$, corresponding to magnetic fields of about $0.5B_{c2}$ and $0.04B_{c2}$, respectively. The dots are numerical solutions of the Eilenberger equations, the dashed line shows the Doppler shift result, the dotted line the result from the method due to Brandt et al, and the solid line the approximate analytical result described in the text.

not surprising, because the Doppler shift method neglects any contributions from vortex core scattering, while the methods AA and BPT are expansions around B_{c2} and are expected to give better results at high fields.

Fig. 6(b) shows the comparison at a considerably smaller field ($\xi/a_\Lambda = 0.2$). In this field range the four methods yield different results, especially close to the gap edge. The numerical result clearly shows Tomasch resonances,⁴² which the other three methods are not able to get. At high energy all methods converge to each other. At low energies, which are especially important for the thermodynamics of the system, the Doppler shift method gives the strongest deviation, while the AA method is closest to the numerical solution.

In Fig. 7 we show the density of states at zero energy as a function of the parameter ξ/a_Λ for both *d*- and *s*-wave superconductor. From these plots it can be seen that in this zero energy limit the AA method appears to

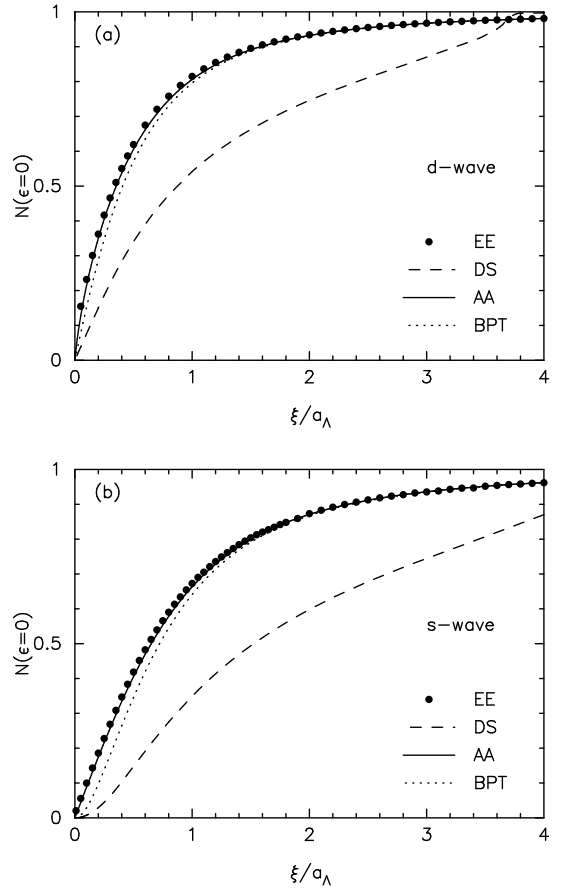


FIG. 7: Zero energy density of states as a function of the parameter ξ/a_Λ for an (a) *d*-wave and an (b) *s*-wave superconductor. The four methods are denoted by the same line patterns as in Fig. 6.

be astonishingly close to the numerical results over the whole field range. At low field the Doppler shift method gives a density of states proportional to ξ/a_Λ for the *d*-wave case, which corresponds to Volovik's $\sqrt{B_{av}}$ law. As seen already in the single vortex case above, the size of the slope turns out to be considerably smaller than in the numerical solution, however. For the *s*-wave case the Doppler shift method and the BPT method both yield a linear B_{av} field dependence at low fields, while the numerical solution and the AA method give a $\sqrt{B_{av}}$ behavior as well. We want to caution, however, that in this field range the Abrikosov vortex lattice Eq. (17), which we were using here, is not an appropriate groundstate wavefunction anymore and important corrections from higher Landau levels are expected.^{43,44} In this field range a fully selfconsistent calculation of the vortex lattice becomes necessary,^{29,45} which will lead to further corrections, like for example the Kramer-Pesch effect⁴⁶ and the vortex core shrinking effect.⁴⁵

V. CONCLUSIONS

We made a detailed comparison of a numerical solution of the quasiclassical Eilenberger equations for *s*- and *d*-wave superconductors in the vortex state with several approximate methods. We studied both the single vortex case and the vortex lattice within a magnetic field directed along the *c*-axis. For the single vortex we found that the Doppler shift method for a *d*-wave gap not only fails in the vortex core region, but also misses important contributions from core states extending into the nodal directions far away from the vortex core. These contributions give important corrections to the density of states especially at low energies, and thus affect the thermodynamics of the system. In particular, corrections to Volovik's law are found, which are expected to be very sensitive to impurity scattering and should be observable via systematic impurity studies of the field dependence of the specific heat. We expect quantum mechanical effects like the Aharonov-Bohm effect to become visible only in very clean samples.

In the vortex lattice there are other approximate methods, which are preferred over the Doppler shift method. Here, we studied two methods which are valid

near the upper critical field B_{c2} : the method due to Brandt, Pesch, and Tewordt and an approximate analytical method, generalizing a method due to Pesch. We showed how the method due to Brandt, Pesch, and Tewordt can be derived from the Eilenberger equations using the Riccati equations. At low fields both of these methods are not able to get the Tomasch resonances, which are present in the numerical solution of the Eilenberger equations. However, especially the approximate analytical method is impressively close to the numerical results at low energies over the whole field range. Since this method is also more convenient than the method due to Brandt, Pesch, and Tewordt, avoiding a solution of an implicit equation and giving analytical results in the clean limit, we recommend the use of this method in the high field range.

Acknowledgments

We would like to thank E. H. Brandt, R. P. Hübener, K. Maki, A. S. Mel'nikov, P. Miranovic, L. Tewordt, and C. C. Tsuei for valuable discussions. Thanks are also due to P. J. Hirschfeld for bringing Ref. 35 to our attention.

¹ Y. Maeno, T. M. Rice, and M. Sigrist, Physics Today **54**, No. 1, p. 42 (2001).

² R. H. Heffner and M. R. Norman, Comments on Cond. Mat. Phys. **17**, 361 (1996).

³ I. J. Lee, S. E. Brown, W. G. Clark, M. J. Strouse, M. J. Naughton, W. Kang, and P. M. Chaikin, Phys. Rev. Lett. **88**, 017004 (2002).

⁴ A. Carrington et al, Phys. Rev. Lett. **83**, 4172 (1999).

⁵ T. R. Kirkpatrick, D. Belitz, T. Vojta, and R. Narayanan, Phys. Rev. Lett. **87**, 127003 (2001).

⁶ S. Haas and K. Maki, Phys. Rev. B **65**, 020502 (2002).

⁷ A. I. Posazhennikova, T. Dahm, and K. Maki, cond-mat/0204272, submitted to Europhys. Lett.

⁸ A. Y. Liu, I. I. Mazin, and J. Kortus, Phys. Rev. Lett. **87**, 087005 (2001).

⁹ G. E. Volovik, JETP Lett. **58**, 469 (1993).

¹⁰ N. Schopohl and K. Maki, Phys. Rev. B **52**, 490 (1995).

¹¹ Y. Wang and A. H. MacDonald, Phys. Rev. B **52**, R3876 (1995).

¹² S. H. Simon and P. A. Lee, Phys. Rev. Lett. **78**, 1548 (1997).

¹³ Y. Morita, M. Kohmoto, and K. Maki, Phys. Rev. Lett. **78**, 4841 (1997).

¹⁴ D. Knapp, C. Kallin, and A. J. Berlinsky, Phys. Rev. B **64**, 014502 (2001).

¹⁵ E. Schachinger and J. P. Carbotte, Phys. Rev. B **62**, 592 (2000).

¹⁶ I. Vekhter, P. J. Hirschfeld, and E. J. Nicol, Phys. Rev. B **64**, 064513 (2001).

¹⁷ K. A. Moler, D. L. Sisson, J. S. Urbach, M. R. Beasley, A. Kapitulnik, D. J. Baar, R. Liang, W. N. Hardy, Phys. Rev. B **55**, 3954 (1997).

¹⁸ M. Franz and Z. Tesanovic, Phys. Rev. B **60**, 3581 (1999).

¹⁹ H. Won and K. Maki, Europhys. Lett. **54**, 248 (2001).

²⁰ K. Maki in *Superconductivity*, ed. R. D. Parks, Marcel Dekker (New York 1969).

²¹ K. A. Moler, D. J. Baar, J. S. Urbach, R. Liang, W. N. Hardy, A. Kapitulnik, Phys. Rev. Lett. **73**, 2744 (1994).

²² B. Revaz, J.-Y. Genoud, A. Junod, K. Neumaier, A. Erb, E. Walker, Phys. Rev. Lett. **80**, 3364 (1998).

²³ D. A. Wright, J. P. Emerson, B. F. Woodfield, J. E. Gordon, R. A. Fisher, and N. E. Phillips, Phys. Rev. Lett. **82**, 1550 (1999).

²⁴ Y. Wang, B. Revaz, A. Erb, A. Junod, Phys. Rev. B **63**, 094508 (2001).

²⁵ G. Eilenberger, Z. Phys. **214**, 195 (1968).

²⁶ A. I. Larkin and Yu. N. Ovchinnikov, Zh. Eksp. Teor. Fiz. **55**, 2262 (1968) - engl. transl. Sov. Phys. JETP **28**, 1200 (1969).

²⁷ J. W. Serene and D. Rainer, Phys. Rep. **101**, 221 (1983).

²⁸ N. Schopohl in *Quasiclassical methods in the Theory of Superconductivity and Superfluidity*, by D. Rainer and J.A. Sauls (eds.), Bayreuth, Germany 1998 (cond-mat/9804064).

²⁹ M. Ichioka, N. Hayashi, N. Enomoto, and K. Machida, Phys. Rev. B **53**, 15316 (1996).

³⁰ M. Franz and Z. Tesanovic, Phys. Rev. Lett. **80**, 4763 (1998).

³¹ K. Yasui and T. Kita, Phys. Rev. Lett. **83**, 4168 (1999).

³² A. S. Mel'nikov, Phys. Rev. Lett. **86**, 4108 (2001).

³³ M. Chiao et al, Phys. Rev. B **62**, 3554 (2000).

³⁴ W. Pesch, Z. Phys. B **21**, 263 (1975); P. Klimesch and W. Pesch, J. Low Temp. Phys. **32**, 869 (1978).

³⁵ I. Vekhter and A. Houghton, Phys. Rev. Lett. **83**, 4626 (1999).

³⁶ see the operator techniques in N. Schopohl, J. Low Temp.

³⁷ Phys. **41**, 409 (1980).

³⁸ M. Abramowitz and I. A. Stegun, *Handbook of mathematical functions*, chapter 7, Dover (New York 1972).

³⁸ U. Brandt, W. Pesch and L. Tewordt, Z. Physik **201**, 209 (1967).

³⁹ H. Won and K. Maki, Phys. Rev. B **53**, 5927 (1996).

⁴⁰ L. Tewordt and D. Fay, Phys. Rev. B **64**, 024528 (2001).

⁴¹ see also the discussion in J. M. Delrieu, J. Low. Temp. Phys. **6**, 197 (1972).

⁴² W. J. Tomasch, Phys. Rev. Lett. **15**, 672 (1965); **16**, 16 (1966).

⁴³ see for example the review by E. H. Brandt, Rep. Prog. Phys. **58**, 1465 (1995).

⁴⁴ E. H. Brandt, J. Low. Temp. Phys. **24**, 409 (1976); Phys. Stat. Sol. B **77**, 105 (1976).

⁴⁵ M. Ichioka, M. Takigawa, and K. Machida, in *Vortices in unconventional superconductors and superfluids*, by R. P. Huebener, N. Schopohl and G. E. Volovik (eds.), Springer Series in Solid-State Sciences, vol. 132 (2001).

⁴⁶ L. Kramer and W. Pesch, Z. Phys. **269**, 59 (1974).